BULLETIN OF THE POLISH ACADEMY OF SCIENCES
TECHNICAL SCIENCES, Vol. 62, No. 4, 2014
DOI: 10.2478/bpasts-2014-0091

Changes of tribological properties of Inconel 600 after ion implantation process

M. BARLAK[1*], M. CHMIELEWSKI[2], Z. WERNER[1], P. KONARSKI[3], K.PIETRZAK[2], and A. STROJNY-NĘDZA[2]

[1] National Centre for Nuclear Research, 7 Andrzeja Sołtana St., 05-400 Otwock, Poland
[2] Institute of Electronic Materials Technology, 133 Wólczyńska St., 01-919 Warsaw, Poland
[3] Tele and Radio Research Institute, 11 Ratuszowa St., 03-450 Warsaw, Poland

Abstract. Commercial Inconel 600 nickel-chromium alloy was implanted with nitrogen, titanium, chromium, copper with tin (as bronze components) and yttrium ions to doses ranging from 1.6e17 to 3.5e17 cm^{-2}. The aim of this research was to investigate the properties of the modified alloy in the context of its application in foil bearings. The virgin and the treated samples were tribologically tested and examined by Scanning Electron Microscopy, Glow Discharge Mass Spectrometry and Energy Dispersive Spectroscopy. The technological studies were preceded by modelling of concentration values of the introduced elements. The results obtained with the use of ion implantation are discussed. There are two advantages which should be highlighted: good agreement in modelling and experimental results of depth profiles of implanted ions, wear resistance improvement of Inconel 600 surface by implantation of copper and tin ions. The tribological tests indicate that abrasion and corrosion are the predominant mechanisms of surface wear.

Key words: foil bearings, ion implantation, Inconel 600, friction coefficient.

1. Introduction

A continuous increase in ecological awareness takes place in parallel with rapid technical and technological progress, which necessitates designing and manufacturing new advanced materials and low-energy structures based on these materials [1–6]. Micro-turbines, and in particular their basic component, i.e. a foil bearing, are a perfect example of such constructions.

Foil bearings can be described as modern aerodynamic bearings, which are widely used in fluid-flow machines constructed applying oil-free technology. Among currently known and classified high-speed bearings, they seem to be one of the most interesting alternatives for both fluid bearings and rolling bearings, which would have a wide range of applications, for instance in complex high-speed and high-temperature turbo-compressors and power micro-turbines. Since foil bearings are not based on oil, it is possible for them to work at temperatures around several hundred Celsius degrees, and in comparison with solutions with rolling bearings, only the rotor's strength can limit the rotational speed of a given instrument.

Figure 1 presents an exemplary structure of a foil bearing. In this bearing, a classic thick-walled liner is covered with a set of foils, including the bump foil and the top foil. The assembly of mating foils is characterized by a low stiffness and has good silencing properties. This ensures excellent operating conditions for the said bearing even at high rotational speed. The function of the bump foil, irrespective of its shape, includes transmitting the loads linked with the rotation of the shaft. On the other hand, the major role of a top foil is to minimize a frictional resistance between it and the shaft neck. The possibility of controlling the properties of the abovementioned set of foils by choosing appropriate materials, thickness and shape of foil should be treated as an advantage of the presented solution. Another crucial feature of such bearings is the shape of the oil clearance (bounded on one side by a structure of great flexibility), which can be adjusted depending on the conditions in the bearing during its operation.

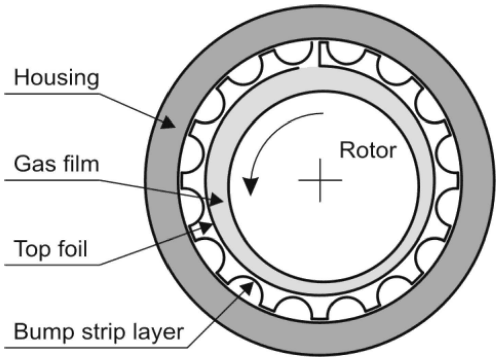

Fig. 1. Schematic design of a foil bearing

Materials used in foil bearings have to meet a number of requirements including, tribological wear observed for the run-up, coasting and overload of the machine. Therefore, materials to be used as bump foil ought to have a high limit of elasticity, enable forming complex shapes and be environmentally resistant (e.g. be corrosion-proof), whereas materials to be used as the top foil should be characterized by high wear resistance, low coefficient of friction, relatively high thermal

*e-mail: Marek.Barlak@ncbj.gov.pl

conductivity and corrosion resistance. It is reasonable to conclude that it would be rather hard for any of the already applied conventional materials to meet all abovementioned conditions at the same time. The materials most often listed in literature, include steel, alloys of copper, nickel, alloys of nickel and plastic [7]. Inconel 600 is also one of possible candidates to be used in this case. It is an alloy of nickel and chromium characterized by satisfactory oxidation resistance at high temperatures and high stress corrosion cracking resistance in a chloride ion environment and corrosion resistance in a caustic soda environment.

As a result of growing requirements set by designers of bearings, traditional materials fail to satisfy these expectations and, as a consequence, it is necessary to either manufacture new materials or modify the surface of those generally accessible [8, 9].

Ion implantation is one of various methods, which can be used for introduction of additional element to the near surface area. This technique is widely used to modify the materials' surface properties for different purposes e.g. to change the tribological properties or to improve the wettabillity of materials [10–12].

There are relatively few reference data on the improvement of tribological properties of Inconel 600. In the literature we can find several examples of ion implantation to the alloys, which are chemically similar to the Inconel 600. There are e.g. alloys: AISI P20, AISI 316, AISI 420, ASSAB 718, NC-6 steel, 34S, 37HS, Inconel 601, Ti-6Al-4V [13–18].

In this paper, we presented the effects of ion implantation of selected elements on a changing of tribological properties of Inconel 600 alloy.

This paper is an extension of our previous publications [19, 20].

2. Experimental

2.1. Modelling. The technological studies were preceded by modelling of the values of main parameters of the ion implantation processes, i.e. the projected range, the range straggling, the sputtering yield and the profiles of the implanted elements, using SUSPRE code [21].

The modelling process was performed for following parameters:

- chemical composition of the substrate: 72Ni-17Cr-11Fe – the concentration was similar to the concentration of these elements in the alloy,
- density of the substrate: 8.47 g/cm^3 (density of real material),
- acceleration voltage: 65 kV,
- implanted elements: N, Ti, Cr, Cu+Sn and Y,
- charge multiplicity: 1.0 for N, 1.9 for Cu, 1.5 for Sn, 2.0 for Ti, 2.0 for Cr and 2.2 for Y,
- beam current: from 1 μm/cm^2 to 1 mA/cm^2,
- ion solubility: 2/target atom (defaults),
- High Dose Effect model: Bucket Fill. The BUCKET model describes the build-up of material like a filling bucket i.e. the implant is accumulated in the target as if it were a filling bucket and while the concentration is lower than the saturation level it will continue to fill unaware of the saturation level. At higher concentrations the implant is lost from the saturated regions.

2.2. Samples. Samples were cut from commercial nickel-chromium Inconel 600 alloy in the form of coupons of $50\times50\times0.1$ mm^3 in size. The chemical composition of Inconel 600 (wt.%) is: min. 72.0 Ni + Co, 14.0–17.0 Cr, 6.0–10.0 Fe, max. 0.15 C, max. 1.0 Mn, max. 0.015 S, max. 0.50 Si and max. 0.50 Cu.

The values of the selected physical and mechanical properties of this alloy are: density: 8.47 g/cm^3, melting range: 1354–1413°C, thermal expansion for the range 21–93°C: 13.3e-6/°C, tensile strength: 655 MPa, proof strength: 310 MPa, elongation: 40% and hardness: 75 HRB [22].

Before processing, the samples were washed in high purity acetone under ultrasonic agitation.

2.3. Processing. Nitrogen, titanium, chromium, copper and tin (as bronze components) and yttrium ions were implanted into Inconel 600 coupons using the MEVVA type implanter with direct beam, without mass separation, described in detail elsewhere [23].

To avoid overheating effects, the samples were clamped onto a water-cooled stainless steel plate. In the case of the implantation of metallic ions, the ion current densities were kept below 10 μA/cm^2, so the substrate temperature did not exceed 200°C.

In the case of nitrogen implantation, the current density was in the range from 1 to 2 mA/cm^2. The sample temperature was in the range 300–400°C.

The base pressure in the vacuum chamber was about 2-5e-4 Pa.

Ions were implanted at 65 kV acceleration voltage.

The implanted doses were 2.2e17, 3.5e17, 3.0e17, 2.5e17, 1.6e17 and cm^{-2} for N, Ti, Cr, Cu and Sn and Y respectively. The values of the fluences correspond to the case of no bucket-type saturation of the profiles and were determined in the modelling stage. For such case we may expect that the profiles will not be distorted by saturation. However the sputtering effects can influence the final ion distributions.

The implantation dose of N is relatively low. In this case, we intended to check the influence of the beam current value higher by a factor of about 100–200 in comparison to the remaining cases on the ion implantation results.

Nitrogen of 99.9% purity was used as the working gas and as the source of gaseous ions.

2.4. Characterization. The Glow Discharge Mass Spectrometry method (GDMS) was applied for the depth profile analysis. The samples were sputtered up to the depth of 2 μm from the surface. GDMS depth profile analysis was performed over 1.5 mm diameter spot eroded in argon.

Tribological tests were conducted according to the following procedure. The samples were pressed against a stainless steel ball of 6.5 mm diameter with a force of $F_n = 10$ N.

A holder together with a ball attached to it were set in reciprocating motion driven by an electro-dynamic generator. The two components between which friction appeared slid on one another at a velocity of 5 mm/s. The friction force F_t thus generated was measured with a piezoelectric displacement sensor at a rate of 24 cps. It was induced and recorded in the friction processes for 30.0 min friction time. The friction coefficient was analyzed using a special software. The tribological tests were conducted at a temperature of 24°C and at 30% of air humidity.

The quality of the surfaces of the virgin, implanted and tribologically tested samples, was examined with the use of Scanning Electron Microscopy method (SEM). Also, the width of the sliding tracks was determined by SEM method. The magnification of the observation was $\times$400 and $\times$5000.

The presence of elements in the surface of the sample and in the sliding tracks was verified by Energy Dispersive Spectroscopy method (EDS).

The value of roughness of the investigated samples (before and after ion implantation process) and the profiles of the sliding tracks were determined by mechanical roughness measuring device.

3. Results and discussions

The average value of the roughness of the virgin samples R_a was about 0.09 μm. Practically, this value was the same after ion implantation process for all treated samples. Also, the morphology of the modified samples (not shown here) did not change during the modification process.

Figure 2 presents the results of the modelled (upper diagrams) and the measured (lower diagrams) profiles of the implanted elements. Additionally, the profiles of three main components (i.e. Ni, Cr and Fe) of Inconel 600 were introduced to the "measured" part. The results for the virgin material were presented also in this part, for a comparison with the implanted materials. The profiles of implanted elements were marked by thick lines.

The maxima of the modelled concentrations and the extensions of the profiles of the detection of the implanted elements were marked by the dotted line and extended to the GDMS graphs.

All graphs were arranged in order of the increasing of the atomic mass of the implanted element.

The modelled projected range for N, Ti, Cr, Cu, Sn and Y is 75.84, 47.88, 44.28, 36.1, 19.32 and 30.8 nm, respectively. The range straggling in (nm) for the same implanted elements is 95, 53, 47, 36, 17 and 28, respectively. The peak volume dopant concentrations are 2.11e22, 6.64e22, 6.31e22, 5.55e22, 3.35e22 and 4.29e22 cm^{-2} for N, Ti, Cr, Cu and Sn, Y, respectively. The sputtering yield were 0.78, 4.78, 5.44, 10.14, 7.12 and 12.5 atoms/ion, respectively.

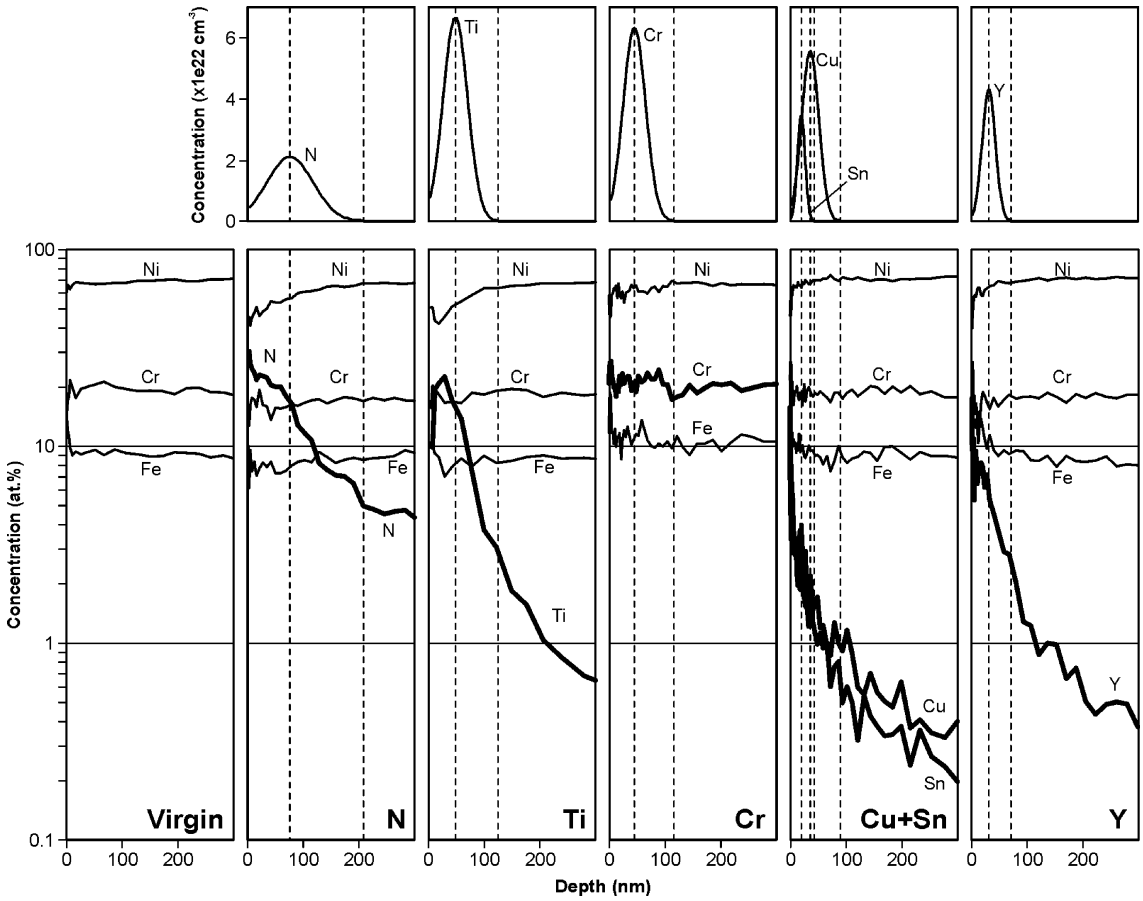

Fig. 2. The results of the modelled and the measured (GDMS) profiles of implanted elements

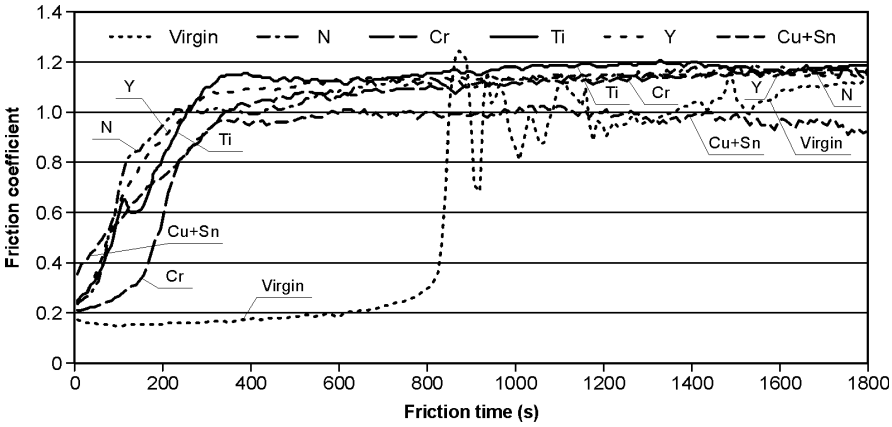

Fig. 3. The change of the friction coefficient vs. time of the tribological tests

We recall that for the case of extended sputtering the maximum retained atomic fraction $C_{\max}$ of the implanted ions for the case when implantation is not too shallow is $C_{\max} = 1/(1 + Y_s)$, where Y_s is the sputtering yield [24].

Therefore, for N, Ti, Cr, Cu and Sn, Y, the maximum retained fractions will be: 0.56, 0.17, 0.15, 0.12, and 0.07, 0.09, respectively.

The measured maximum concentration of the implanted elements are (at.%) about: 30 for N, 25 for Ti, 27 for Cr, 16 for Cu, 12 for Sn and 18 for Y.

The modelled profiles of the introduced elements are shown in comparison with the GDMS profiles. We can see that the latter are in qualitative agreement with our predictions.

Figure 3 shows the change of the friction coefficient vs. time of the tribological tests.

The friction courses can be split in two parts: the first - from start of the measurement to the stabilization of the process (after about 200–300 s for the modified material and after about 1600 s for the "virgin" one) and the second - from the stabilization of the process to the end of the measurement. In the first part we can observe a fast increase in the friction coefficient, in the second – a slow growth or approximately "constant" value (plateau).

There are different ways to reach a constant value. The change for Cu+Sn modified sample has an almost linear character and its value is about 0.0019 s^{-1}. Other situation can be observed for samples modified by Cr, Ti, Y and N. Several (2–4) steps of the change of friction coefficient for each spectra may be distinguished.

The value of the friction coefficient for Cu+Sn modified samples is of the order of 0.95, while this value for other cases is at the level of 1.1 for N and Cr, 1.15 for Ti and 1.13 for Y.

The behaviour of virgin material is different. We can observe a long plateau (about 800 s), and next - large and sudden changes of friction coefficient. Only after 1600 s, the value of friction coefficient is "constant" and it is about 1.1. Probably, this change of the friction coefficient of non-treated material is the result of the destruction of the surface oxide layer, which protects the surface of the alloy from the corrosion and which was not modified by additional elements. We try to explain this phenomenon as follows. The thickness of the oxide layer on Inconel 600 is a few hundred nanometers in normal conditions – typically to 0.3–0.35 μm [25]. The depth of the typical pits on the virgin material after tribological tests was about 1 μm. The medium rate of the wear of this material was about 5.56e-4 μm/s. After 800 s of the process, the wear depth was about 0.44 μm. We believe, that in this time, the oxide layer was broken and e.g. the processes of the oxidation of the alloy components induce a change of the kinetics of the wear process.

Figure 4 shows the selected (for N, Ti and Y implanted ions) results of SEM observations of the character of the typical sliding tracks for the modified samples. For better visualization of the surface changes, the "compo" (composition) and "topo" (topography) modes were used.

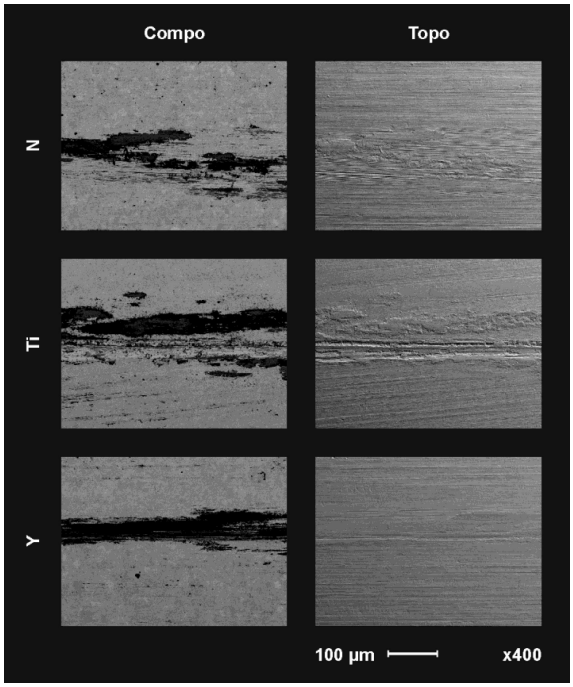

Fig. 4. The selected results of SEM observations of the sliding tracks on the surface of the modified samples of Inconel 600

The measured width of sliding track, determined by SEM observations is about: 132 μm for virgin material, 124 μm for N, 112 μm for Cr and Ti, 76 μm for Y and 68 μm for Cu+Sn implantations, respectively.

The SEM observation results show also, that in all cases, the wear track after tribological tests is not a classical groove. The morphology of all tracks exhibits grooves parallel to the sliding direction and sometimes the cracks. Additionally, in the case of: virgin, N, Cr and Ti ion implanted samples, the particles of the removed material embedded within the substrates are observed. A lot of these particles is observed particularly in the virgin and N-modified samples. The sliding tracks on the Y and Cu+Sn implanted samples have different character and practically only parallel grooves are visible.

This morphology of the investigated samples indicates the typical abrasive nature of the wear (which is observed when a harder material is rubbing against a softer one) in the microploughing wear mode. In this case, the material is shifted to the sides of the wear groove and it is not removed from the surface. The cracks in some samples may suggest additional micro-cracking (brittle fracture) mode, in which the material cracks in the subsurface regions surrounding the wear groove [26]. Examples of this wear were described, e.g. in [27, 28].

Generally, in our systems, "two body abrasive wear" is present, because there are only two rubbing components involved in the friction process. However, the presence of the embedded particles suggests the occurrence of "three body abrasive wear", which is characterized by hard particles trapped between the rubbing surfaces. Hard particles of iron oxides could be a "third body" in our case.

Figure 5 shows SEM and EDS results for samples implanted with Ti and with Y. The magnification of the presented observations results is $\times$400 in titanium and yttrium case and additionally $\times$5000 in yttrium case.

We can see the presence of the strong signal from iron and oxygen in the sliding grove region for both modification cases. The EDS mapping results suggest the occurrence of the process of iron oxidation in the investigated systems. The appearance of Fe-O phases in the system suggests additional new mechanism of wear. Apart from the abrasive wear this is the corrosive wear mechanism [26].

Additionally, in Fig. 5, the previously mentioned cracks in Y implanted samples are visible at SEM image with the magnification of $\times$5000. These cracks are in the sliding grove. The light lines on the left side of described image are the tracks of the previous production process of the plates.

EDS mapping results for Y implanted samples show that the introduced yttrium is present in all observed area (also in the sliding grove) in the similar concentration. The presence of titanium in the sliding grove is not so clear.

SEM and EDS results presented for Ti implanted samples vary similarly to the results obtained for virgin samples and for the samples implanted with N and Cr. The same correlation was observed for the samples implanted with Y and Cu+Sn.

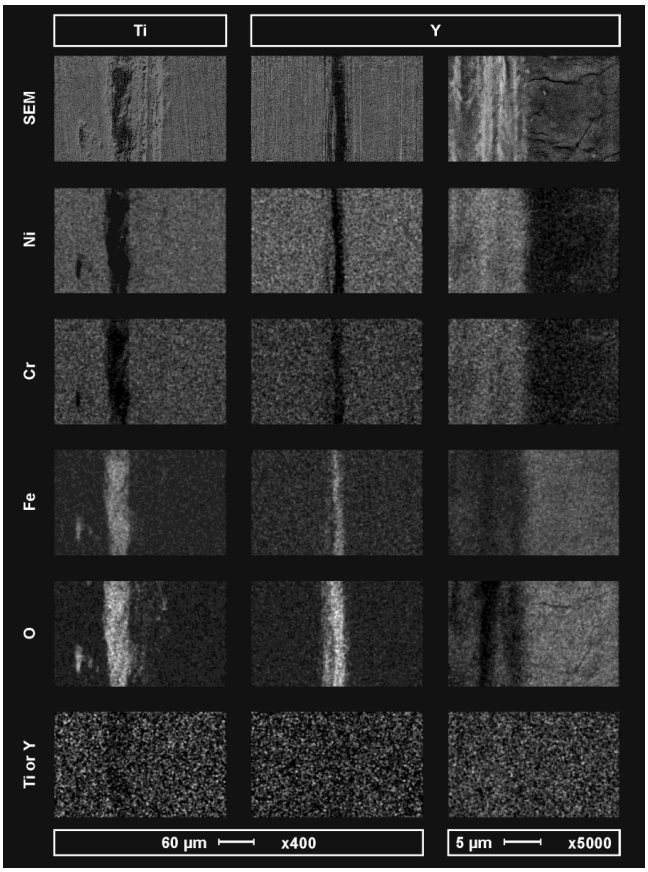

Fig. 5. The selected EDS results of the sliding tracks on the surface of the modified samples of Inconel 600

Figure 6 shows the selected profiles of the sliding tracks. All measured profiles of the individual sliding tracks correspond exactly to the results of the microscopic observations.

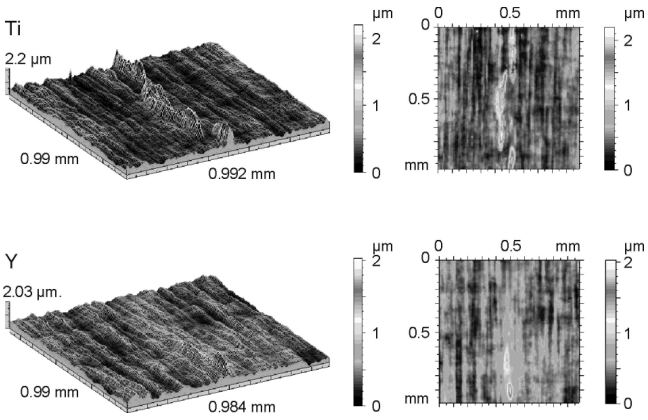

Fig. 6. The selected profilograms of the surfaces with the wear tracks

The shape of wear tracks in the virgin, N, Cr and Ti ion implanted samples confirms the presence of both the grooves and the embedded particles. The maximum distance between the pits and the peaks is up to more than 2 μm. The surfaces of the samples modified by Y and Cu+Sn have different character. The shape of these surfaces is more smooth, without large grooves and large peaks. The surface of Cu+Sn ion implanted samples is particularly homogeneous.

Comparing EDS results and profilograms, it can be concluded that in selected cases, the depth and the influence of the occurrence of the implanted elements is greater than the depth modelled in SUSPRE code. It is observed for example for Y and Cu+Sn modifications. Such phenomenon is known in the surface modification, especially for nitrogen ion implantation. In our case, it is particularly valuable, because tin has lubricating properties, which are visible in Fig. 3 (small and constant values of coefficient, a mild course of the tribological test).

At this moment, it is not known what mechanism (stresses, diffusion, Soret effect, temperature of modified samples, temperature of investigated samples, defects of structure, "rubbing" of element) is dominant in the investigated systems.

4. Conclusions

The tribological effects of N, Cr, Ti, Y and Cu + Sn ion implantation in Inconel 600 using a stainless steel ball were investigated. On the basis of the obtained results, it can be concluded that:

1. For proposed parameters, the processes of ion implantation have no influence on the roughness value and the surface morphology of the modified samples.
2. Although, the modelling of the multi-component systems is a very difficult procedure, which ignores many phenomena, it can be used to the first approximation of the evaluation of the parameters of the ion implanted alloys, like Inconel 600.
3. In all cases, the wear track after tribological tests is not a classical groove but a series of individual grooves can be observed.
4. The tribological tests and EDS measurements indicate predominantly abrasive (in micro-ploughing mode and microcracking mode) and corrosive mechanism of the wear.
5. The tribological tests show that the value of friction coefficient of the virgin material after stabilization process is very similar to the values of the friction coefficient for Inconel 600 samples implanted with N, Ti, Cr and Y, however the kinetics of the wear process of these materials are very different,
6. The wear process of the virgin samples of Inconel 600 is unstable and therefore, the use of the non-modified material may be problematic; it appears that this material can be used in the systems with the mild loads,
7. The wear process of Inconel 600 samples implanted with Cu+Sn ions has other character:
   - the process is very stable,
   - it includes only 2 steps with practically the linear character,
   - the value of friction coefficient is the smallest of the all cases; it is about 15% smaller in comparison to other cases,
   - the sliding track is different (softer) in comparison to the sliding tracks on virgin material and on the materials implanted with N, Ti and Cr, and very similar to the track on Y implanted samples,
   - a comparison of the wear results with the results of other investigations shows that "good" effect (lubrication) of Cu+Sn modification is observed at depths, which are greater than the implantation range for both elements,
   - the retained doses of Cu and Sn are among the smallest of the implanted ions,
   - at this moment, the individual influences of Cu and Sn are unknown; this influence should be investigated in the nearest future.

Concluding our studies show that Cu+Sn implantation gives the best results among all proposed cases.

Acknowledgements. The results presented in this paper have been obtained within the project "Using intelligent materials and structures to develop and implement the concept of the innovative bearing system in power microturbine rotors" (contract no. UDA-POIG.01.03.01-00-027/08-00 with the Polish Ministry of Science and Higher Education) within the framework of the Operational Programme Innovative Economy 2007–2013.

The authors wish to thank Mr. J. Zagórski for technical assistance.

REFERENCES

[1] V.K. Lindroos and M.J. Talvitie, "Recent advances in metal-matrix composites", *J. Materials Processing Technology* 53, 273–284 (1995).

[2] W. Węglewski, M. Basista, M. Chmielewski, and K. Pietrzak, "Modelling of thermally induced damage in the processing of Cr-Al_2O_3 composites", *Composites Part B: Engineering* 43, 255–264 (2012).

[3] M. Chmielewski and W. Weglewski, "Comparison of experimental and modelling results of thermal properties in Cu-AlN composite materials", *Bull. Pol. Ac.: Tech.* 61 (2), 507–514 (2013).

[4] K. Pietrzak, W. Olesinska, D. Kalinski, and A. Strojny-Nedza, "The relationship between microstructure and mechanical properties of directly bonded copper-alumina ceramics joints", *Bull. Pol. Ac.: Tech.* 62 (1), 23–32 (2014).

[5] J. Zimmerman, Z. Lindemann, D. Golański, T. Chmielewski, and W. Włosiński, "Modeling residual stresses generated in Ti coatings thermally sprayed on Al_2O_3 substrates", *Bull. Pol. Ac.: Tech.* 61 (2), 515–525 (2013).

[6] A. Krajewski, W. Włosiński, T. Chmielewski, and P. Kołodziejczak, "Ultrasonic-vibration assisted arc-welding of aluminum alloys", *Bull. Pol. Ac.: Tech.* 60 (4), 841–852 (2012).

[7] C.-P.R. Ku and H. Heshmat, "Compliant foil bearing structural stiffnes analysis – Part II: Experimental investigations", *J. Tribology* 115, 364–369 (1993).

[8] T. Chmielewski and D. Golański, "New method of in-situ fabrication of protective coatings based on Fe-Al intermetallic compounds", *J. Engineering* B 225, 611–616 (2011).

[9] W. Wlosinski and T. Chmielewski, "Plasma-hardfaced chromium protective coatings-effect of ceramic reinforcement on their wettability by glass", *Proc. 3rd Int. Conf. Surface Engineering* 1, 48–53 (2002).

[10] J. Piekoszewski, W. Olesinska, J. Jagielski, D. Kalinski, M. Chmielewski, Z. Werner, M. Barlak, and W. Szymczyk, "Ion implanted nanolayers in AlN for direct bonding with copper", *Solid State Phenomena* 99–100, 231–234 (2004).

[11] M. Barlak, J. Piekoszewski, J. Stanislawski, Z. Werner, K. Borkowska, M. Chmielewski, B. Sartowska, M. Miskiewicz, W. Starosta, L. Walis, and J. Jagielski, "The effect of intense plasma pulse pre-treatment on wettabillity in ceramic-copper system", *Fusion Engineering and Design* 82, 2524–2530 (2007).

[12] M. Barlak, W. Olesińska, J. Piekoszewski, Z. Werner, M. Chmielewski, J. Jagielski, D. Kaliński, B. Sartowska, and K. Borkowska, "Ion beam modification of ceramic component prior to formation of AlN-Cu joints by direct bonding process", *Surface and Coatings Technology* 201, 8317–8321 (2007).

[13] J.P. Rivière, P. Méheust, J.A. García, R. Martínez, R. Sánchez, and R. Rodríguez, "Tribological properties of Fe and Ni base alloys after low energy nitrogen bombardment", *Surface and Coatings Technology* 158–159, 295–300 (2002).

[14] K.L. Dahma, K.T. Short, and G.A. Collins, "Characterisation of nitrogen-bearing surface layers on Ni-base superalloys", Short communication, *Wear* 263, 625–628 (2007).

[15] J.F. Lin, K.W. Chen, J.Q. Xie, C.C. Wei, J.C. Chung, M.Y. Li, and C.-F. Ai, "Effects of implantation temperature and volume flow rate ratio of nitrogen and hydrogen on nitrogen concentration distribution, mechanical properties, fatigue life, fracture toughness, and tribological behavior of plasma-nitrided P20, 718 and 420 steels", *Surface and Coatings Technology* 201, 5912–5924 (2007).

[16] Z. Werner, J. Piekoszewski, R. Grötzschel, and W. Szymczyk, "Implantation of steel from MEVVA source with bronze cathode", *Emerging Applications of Vacuum-Arc-Produced Plasma, Ion and Electron Beams* 88, 187–190 (2002).

[17] P. Budzynski, A.A. Youssef, and B. Kamienska, "Influence of nitrogen and titanium implantation on the tribological properties of steel", *Vacuum* 70, 417–421 (2003).

[18] J.I. Oñate, F. Alonso, and A. García, "Improvement of tribological properties by ion implantation", *Thin Solid Films* 317, 471–476 (1998).

[19] M. Chmielewski, M. Barlak, K. Pietrzak, D. Kaliński, E. Kowalska, and A. Strojny-Nędza, "Tribological effects of ion implantation of Inconel 600", *Nukleonika* 57 (3), 357–362 (2012).

[20] P. Konarski, K. Kaczorek, D. Kaliński, M. Chmielewski, K. Pietrzak, and M. Barlak, "Ion implanted inconel alloy – SIMS and GDMS depth profile analysis", *Surface and Interface Analysis* 45, 494–497 (2013).

[21] SUSPRE, www.surrey.ac.uk/ati/ibc/research/modelling_simulation/suspre.htm.

[22] Inconel® alloy 600, W.No.2.4816, www.bibusmetals.com.pl.

[23] S.P. Bugaev, A.G. Nikolaev, E.M. Oks, P.M. Schanin, and G.Y. Yushkov, "The "TITAN" ion source", *Review of Scientific Instruments* 65, 3119–3125 (1994).

[24] H. Ryssel, "Range distributions", in *Ion Implantation Techniques*, ed. H. Glawischnig, pp. 177–193, Springer, Berlin, 1982.

[25] A. Haouam, K. Dawi, and B. Merzoug, "Thermodynamic modeling of the surface layer structure on Inconel 600 oxidized in a controlled atmosphere", *Scientific Study and Research – Chemistry and Chemical Engineering, Biotechnology, Food Industry* 13 (1), 91–104 (2012).

[26] D. Kopeliovich, "Mechanisms of wear", www.substech.com/dokuwiki/doku.php?id=mechanisms_of_wear (2009).

[27] C. Ionescu, M. Abrudeanu, P. Ponthiaux, F. Wenger, and V. Rizea, "Effect of normal force on tribocorrosion behaviour of Ni-30Cr model alloy in LiOH-H_3BO_3 solution" *Revue Roumaine de Chimie* 56, 907–915 (2011).

[28] L.C. Julián and A.I. Muñoz "Influence of microstructure of HC CoCrMo biomedical alloys on the corrosion and wear behaviour in simulated body fluids" *Tribology Int.* 44, 318–329 (2011).